ISPRS Journal of Photogrammetry and Remote Sensing ▮ (▮▮▮▮) ▮▮▮–▮▮▮

Contents lists available at ScienceDirect

ISPRS Journal of Photogrammetry and Remote Sensing

journal homepage: www.elsevier.com/locate/isprsjprs

Assessment of radargrammetric DSMs from TerraSAR-X Stripmap images in a mountainous relief area of the Amazon region

Cleber Gonzales de Oliveira *, Waldir Renato Paradella, Arnaldo de Queiroz da Silva

National Institute for Space Research (INPE), Remote Sensing Division (DSR), Av. dos Astronautas, 1.758, Jd. da Granja, CEP: 12227-010, São José dos Campos-SP, Brazil

ARTICLE INFO

Article history:
Received 31 August 2009
Received in revised form
19 August 2010
Accepted 25 August 2010
Available online xxxx

Keywords:
DSM
TerraSAR-X Stripmap
Topographic mapping
Brazilian Amazon

ABSTRACT

The Brazilian Amazon is a vast territory with an enormous need for mapping and monitoring of renewable and non-renewable resources. Due to the adverse environmental condition (rain, cloud, dense vegetation) and difficult access, topographic information is still poor, and when available needs to be updated or re-mapped. In this paper, the feasibility of using Digital Surface Models (DSMs) extracted from TerraSAR-X Stripmap stereo-pair images for detailed topographic mapping was investigated for a mountainous area in the Carajás Mineral Province, located on the easternmost border of the Brazilian Amazon. The quality of the radargrammetric DSMs was evaluated regarding field altimetric measurements. Precise topographic field information acquired from a Global Positioning System (GPS) was used as Ground Control Points (GCPs) for the modeling of the stereoscopic DSMs and as Independent Check Points (ICPs) for the calculation of elevation accuracies. The analysis was performed following two ways: (1) the use of Root Mean Square Error (RMSE) and (2) calculations of systematic error (bias) and precision. The test for significant systematic error was based on the *Student's-t* distribution and the test of precision was based on the *Chi-squared* distribution. The investigation has shown that the accuracy of the TerraSAR-X Stripmap DSMs met the requirements for 1:50,000 map (Class A) as requested by the Brazilian Standard for Cartographic Accuracy. Thus, the use of TerraSAR-X Stripmap images can be considered a promising alternative for detailed topographic mapping in similar environments of the Amazon region, where available topographic information is rare or presents low quality.

1. Introduction

Approximately 60% of the Amazon forest lies in Brazil. The Brazilian Amazon with a continental dimension (5217,423 km^2) concentrates, under an apparently homogeneous physiognomy, an enormous variability in forests, rivers and lakes, soils, geology, climate, plants and animals (Schubart, 1989). Many obstacles have been faced for the integration of the Brazilian Amazon region to the rest of the country. This integration is necessary nowadays more than ever in view of increase in Brazilian population, the immense natural resources available in the region and the country's sovereignty.

Government infrastructure planning, resources assessment, monitoring and management are based on geospatial information. The lack of reliable information impairs the ability of the government to formulate policies, establish priorities and perform essential activities like regulate colonization and exploitation of natural resources in ecologically sensitive areas. The primary inputs supporting all geographic information are topographic maps. Due to adverse environmental conditions (rain, cloud, smoke, dense vegetation, poor access), the usage of optical remote sensing data for regular basis coverage is expensive or not even possible. As a consequence, the Brazilian topography is poorly known, with only 15% of the area covered by maps at detailed scale (1:50,000). In addition, this topographic information when available is outdated and needs to be updated or re-mapped (IBGE, 2002). Digital Surface Model (DSM) represents the elevation of the top surface of vegetation cover and other features (buildings, manmade structures, etc.) above the bare earth (Maune, 2007). DSM is also a primary input for topographic mapping. With the launch of RADARSAT-1 in 1995, DSMs could be for the first time systematically generated using stereo pair of Synthetic Aperture Radar (SAR) orbital images (radargrammetry). The generation of a DSM by radargrammetry is a process which aims at the reconstruction of a three dimensional terrain surface using a stereoscopic pair of SAR images. The quality of the resultant DSM is largely dependent on the SAR stereo configuration and the accuracy of the measured parallaxes (Li et al., 2006). Results have been published with RADARSAT-1 stereo images in the Brazilian

* Corresponding author. Tel.: +55 12 3208 6732; fax: +55 12 3208 6488.
E-mail addresses: cleber@dsr.inpe.br (C.G. Oliveira), waldir@dsr.inpe.br (W.R. Paradella), arnaldo@dsr.inpe.br (A.Q. Silva).

0924-2716/$ – see front matter © 2010 International Society for Photogrammetry and Remote Sensing, Inc. (ISPRS). Published by Elsevier B.V. All rights reserved.
doi:10.1016/j.isprsjprs.2010.08.008

Amazon with a general consensus: RMSE (Root Mean Square Error) around 15 m for flat terrain and 20 m for mountainous relief (Oliveira and Paradella, 2008; Paradella et al., 2005). In addition, the altimetry produced from SRTM3 (3-arc seconds by 3-arc seconds) indicated an average error of 12 m in elevation for flat and mountainous terrains (Oliveira and Paradella, 2008).

The classification of topographic maps in Brazil should be performed in accordance to the National Cartographic Accuracy Standard (PEC in Portuguese), established by the Brazilian Cartographic Commission. PEC is a statistical indicator (90% of probability) for planialtimetric accuracy, corresponding to 1.6449 times the RMSE (PEC = 1.6449 × RMSE). For a 1:50,000 scale A Class Map, the altimetric RMSE corresponds to 6.67 m (1/3 of the equidistance of contour lines). Based on previous results neither altimetry produced from interferometry (SRTM3) nor from SAR stereoscopy (RADARSAT-1) fulfilled the altimetric PEC requirements for detailed topographic mapping (1:50,000) in the Brazilian Amazon. This study is an outgrowth of previous researches of the authors focusing on the use of orbital SAR stereo pairs to overcome the critical lack of topographic information in the Brazilian Amazon (Oliveira and Paradella, 2008, 2009; Paradella et al., 2005). The altimetric quality of DSMs generated from TerraSAR-X Stripmap stereo data was evaluated for a mountainous topographic terrain in the Carajás Province and it shows a practical example of how the altimetry provided by the German SAR can be applied to overcome the critical lack of detailed topographic information in the Amazon region.

2. Study area

The test-site encompasses the Parauapebas municipality (Pará State) with almost 1350 km^2 (Fig. 1). It is within the Carajás Province, the most important Brazilian mineral province with the world's largest iron deposits and important deposits of copper, gold, manganese, nickel, among others (Paradella et al., 1997). The region is characterized by a set of hills and plateaus (altitudes from 500 to 900 m) surrounded by southern and northern lowlands (altitudes around 200 m), totally covered by Ombrophilous Equatorial forest (Paradella et al., 1994). It comprises part of Caldeirão and Serra dos Carajás topographic sheets (1:100,000 scale), the more detailed systematic topographic mapping produced from black and white air photos by the Brazilian Institute of Geography and Statistics (IBGE) during the 1979–1981 period.

3. Dataset

3.1. TerraSAR-X

TerraSAR-X (TSX) was launched on June 15, 2007 and is the first German radar satellite with one meter resolution (Herrmann and Bottero, 2007). The satellite is equipped with a right-side-looking SAR based on active phased array antenna technology and provides high-resolution X-band SAR data in distinct modes: High Resolution Spotlight (HG), Spotlight (SL), Stripmap (SM) and ScanSAR (SC). Each TSX product is a combination of satellite parameters (beam and position) and the level of data processing (Fritz and Eineder, 2009).

The selection of the best stereo-pair for extracting a radargrammetric DSM is a function of sensor (intersection angle, proportion of overlap between beam positions and spatial resolution) and terrain parameters (expected elevation accuracy, size of the study area, elevation, slope and surface characteristics). Considering the options for TSX coverage in the study area, one same-side stereo pair using SM mode in descending orbit (west facing pass) was acquired. Given the capabilities of the sensor and platform, a set of products has been designed taking into account processing algorithms and parameters regarding geometric projection and radiometric resolution. In relation to the geometric projection, the Multi Look Ground Range Detected (MGD) representation was used with reduced speckle and approximately square resolution cells on ground. The scene coordinates are oriented along flight direction and along ground range. The pixel spacing is equidistant in azimuth and ground range. A simple polynomial slant to ground projection is performed in range using a WGS84 ellipsoid and an average, constant terrain height. The advantage of MGD is that no image rotation to a map coordinate system is performed and interpolation artifacts are avoided. In relation to the radiometric resolution, the scenes were delivered as a Spatially Enhanced (SE) product, designed for the highest possible square ground resolution. This combination of TSX products is the best choice for DSM extraction by radargrammetry, because it preserves the best geometric and radiometric characteristics of the data. The intersection angle between the images is almost 19°, enough to obtain good stereo geometry (observed parallax). The pair of images was acquired with five days apart during the dry season, minimizing radiometric variations induced by environmental and phenological changes at the terrain (Table 1).

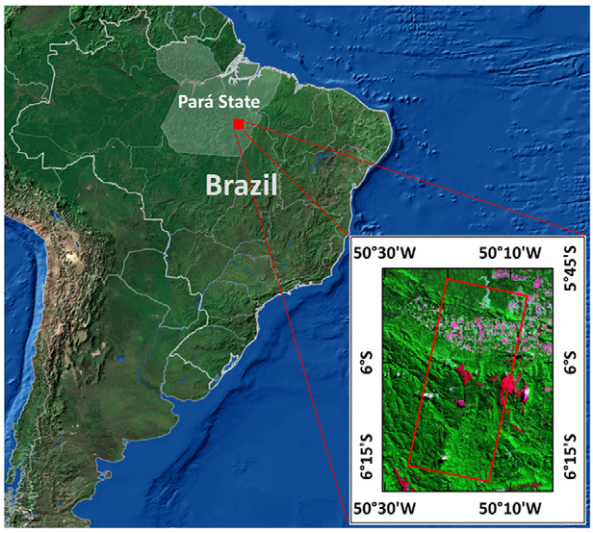

Fig. 1. Location of the study area.

Table 1
TerraSAR-X Stripmap (TSX-SM) images characteristics.

Image code	TSX-SM-745	TSX-SM-916
Product	MGD-SE	MGD-SE
Acquisition date	Dec/04/2008	Nov/29/2008
Look azimuth	282°	282°
Incidence angle (center)	29.48°	48.13°
Pixel spacing (m)	1.25 × 1.25	1.25 × 1.25
Spatial resolution range × azimuth (m)	3.00 × 3.02	3.01 × 3.02

3.2. GPS field measurements

Although the requirements for Ground Control Points (GCPs) numbers are not defined for deriving a radargrammetric DSM, a larger number is recommended to improve accuracy of the product with samples ideally chosen on a variety of locations and ground elevations, particularly at the lowest and highest elevation. On the other hand, Independent Check Points (ICPs) also play a key role in quality control for mapping production. This is a controversial issue since a balance has to be reached between few ICPs, giving invalid accuracy estimation and an excessive number, providing

Please cite this article in press as: Oliveira, C.G., et al., Assessment of radargrammetric DSMs from TerraSAR-X Stripmap images in a mountainous relief area of the Amazon region. ISPRS Journal of Photogrammetry and Remote Sensing (2010), doi:10.1016/j.isprsjprs.2010.08.008

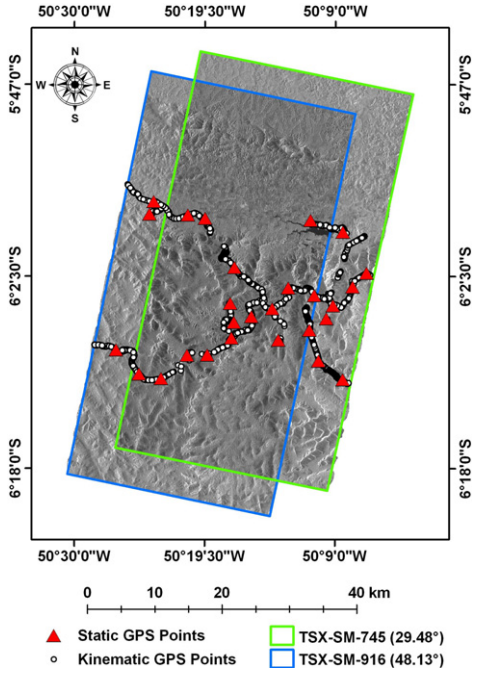

Fig. 2. Distribution of the GPS field measurements over the TerraSAR-X Stripmap stereo-pair.

a safe analysis with unrealistic cost. Based on the literature a minimum of 20 or 28 well-distributed ICPs within a map is normally necessary (Merchant, 1982; USGS, 1997).

Precise planialtimetric measurements from a Global Positioning System (GPS) were acquired in the test-site and used as GCPs for the modeling of the DSMs and as ICPs for the calculation of altimetric accuracies. Two dual frequency geodetic GPS receivers were used in the field for the static GPS measurements and a total of 48 static measurements and 35,000 kinematics measurements were collected during field campaigns using helicopter and vehicle. It is important to mention that due to logistic restriction, the measurements were carried on the ground (sites without vegetation). The maximum errors with a probability of 68.3% (1σ) for the estimated positions were 18 cm (latitude), 75 cm (longitude) and 24 cm (ellipsoidal height) in geodetic coordinates related to the WGS84 ellipsoid. The distribution of the points over the TerraSAR-X stereo-pair is presented in Fig. 2.

4. Methodological approach

4.1. Mathematical models for DSM generation

Two mathematical models have been used for satellite sensor orientation and 3D geo-positioning in the last decades: a rigorous mathematical model (or physical model) and a non-rigorous mathematical model (empirical model). Normally, rigorous mathematical models are more accurate than empirical models because they consider all the sensor information, and the satellite and Earth motion (Shaker, 2008). An example of a 3D physical model is the three-dimensional CCRS physical model that was developed as an integrated and unified geometric modeling to geometrically process SAR images and has also benefited from theoretical work in celestial mechanics to better determine the satellite's oscillatory parameters over long orbit (Toutin et al., 1992). This model was subsequently adapted to RADARSAT-1 images by Toutin (1998, 2000), respectively in the evaluation of the geometric accuracy and evaluation of radargrammetric DSMs of RADARSAT-1 images. This adapted model (Toutin's 3D Radargrammetric) represents the well-known collinearity condition (and coplanarity condition for stereo models), and integrates the different distortions relative to the global geometry of view, including effects relative to the platform, to the sensor, to the Earth and to the cartographic projection. This model is embodied into OrthoEngine photogrammetric software (PCI Geomatics, 2007) and the techniques implemented in this software are presented in Ostrowski and Cheng (2000). The integration and the detailed derivation of the equations, mainly based on the collinearity equations and on radargrammetry, are out of scope of this paper. The final results for SAR images, which link the 3D cartographic coordinates to the image coordinates can be found in Toutin et al. (1992) and Toutin (2003) and is given by:

$$Pp + y(1 + \delta\gamma X) - \tau h = 0 \quad (1)$$

$$X = (\theta h)/(\cos\chi) + \alpha q[Q + \theta X - (h/\cos\chi)] = 0 \quad (2)$$

where

$$X = (x - ay)[1 + (h/N_o)] + by2 + cxy + \delta h h^2. \quad (3)$$

Each parameter is given using a mathematical formula that represents the physical realities of the full-viewing geometry (satellite, sensor, earth, map projection):

- N_o normal distance to the ellipsoid;
- a mainly a function of the nonperpendicularity of axes;
- α field of view for an image pixel;
- p, q image coordinates;
- P, Q scale factors in along-track and across-track directions, respectively;
- τ, θ function of the leveling angles in along-track and across-track directions, respectively;
- x, y, z 3D ground coordinates;
- $b, c, \chi, \delta\gamma, \delta h$ second-order parameters, which are functions of the total geometry, e.g., satellite, sensor, image, and earth.

Each of these parameters is in fact the combination of several correlated variables of the viewing geometry, so that the number of unknown parameters has been reduced to an independent uncorrelated set. The unknown parameters are thus translations (in X and Y) and a rotation related to the cartographic north, the scale factors and the leveling angles in both directions, the nonperpendicularity of axes, as well as some of the second-order parameters when the orbital data are not accurate.

Basically, the following processing steps are necessary to produce a radargrammetric DSM: acquiring stereo-images, collecting GCPs and stereo-model setup, extracting elevation parallaxes and computing 3D coordinates. The SAR images are standard products in slant or ground-range forms, but the latter is normally used since the pixel spacing on the ground is roughly the same for the different look-angle images and this facilitates stereo-viewing and matching. GCPs are needed to refine the stereo-model parameters with a least square bundle adjustment process in order to obtain cartographic-standard accuracy. To extract the elevation parallax two methods can be used by image matching: visual or automatic. The former is an extension of the traditional photogrammetric method and it is a long and expensive process to derive DSMs while automated image matching is straightforward (Toutin and Gray, 2000).

Toutin's 3D Radargrammetric model available at TSX module of OrthoEngine software was used to compute the stereo model and the 3D intersections for the DSM extractions. Once the geometric model was computed, quasi-epipolar images were generated to increase the similarity between the two images; and the elevation parallax was derived based on automated image matching procedure, which uses a standard normalized area-based correlation approach. No speckle filtering was applied in the original TSX-SM images in order to avoid reducing the low relief and decreasing the DSM accuracy (Toutin, 1999).

Please cite this article in press as: Oliveira, C.G., et al., Assessment of radargrammetric DSMs from TerraSAR-X Stripmap images in a mountainous relief area of the Amazon region. ISPRS Journal of Photogrammetry and Remote Sensing (2010), doi:10.1016/j.isprsjprs.2010.08.008

4.2. Accuracy analysis

Accuracy and classification of the products were estimated comparing DSM elevation values and real elevation provided by ICPs. The accuracy analysis was performed following two approaches: (1) the use of Root Mean Square Error (RMSE) for the overall classification of the DSMs considering the PEC limits, and (2) calculations of systematic errors (bias) and precision based on the methodology proposed by Galo and Camargo (1994).

The RMSE is expressed as:

$$\mathrm{RMSE} = \sqrt{\frac{\sum_{i=1}^{n}(z_{\mathrm{DSMi}} - z_{\mathrm{GPSi}})^2}{n}} \tag{4}$$

where z_{DSMi} refers to the ith elevation extracted from TSX-SM DSM, z_{GPSi} refers to the ith elevation measured from GPS, and n is the number of sample points. The normality of the errors can be studied from histograms, dot plots, box plots, and normal probability plots of the residuals. In addition, comparisons can be made of observed frequencies with expected frequencies if normality holds, and formal tests can be utilized (Kutner et al., 2004). The *Shapiro–Wilk* test (Shapiro and Wilk, 1965) is a formal test used to verify if the errors are normally distributed. The null hypothesis for this test is that the data are normally distributed. For an alpha level of 0.05 and the p-value less than 0.05, the null hypothesis is rejected. If the p-value is greater than 0.05, then the null hypothesis has not been rejected.

The systematic error (bias) expresses the tendency of discrepancies to be of the same magnitude and direction, and precision expresses the tendency of discrepancies to follow the characteristics of a normal distribution. The analysis is accomplished by standard statistical procedures on both the sample mean (μ_z) to assess the presence of a significant bias error and on the sample standard deviation (s_z) to assess compliance with precision. The test for significant bias error is based on the *Student-t* distribution and test of precision is based on the *Chi-squared* distribution. Hypothesis testing is performed on μ_z and s_z respectively and both tests are based on a confidence level $(1-\alpha)$ of 95% (Galo and Camargo, 1994).

The tests are made using the discrepancies between the elevations (z) determined from the TSX-SM DSMs and for corresponding ICPs determined from the GPS field measurements. The sample mean of discrepancies (μ_z) is computed as:

$$\mu_z = \frac{1}{n}\sum_{i=1}^{n}\Delta z_i \tag{5}$$

where Δz_i is the residual discrepancies in elevation computed as $\Delta z_i = z_{\mathrm{DSMi}} - z_{\mathrm{GPSi}}$ and n is the number of ICPs.

The sample standard deviation of test point discrepancies (s_z) is computed as:

$$s_z = \sqrt{\left[\frac{1}{n-1}\sum_{i=1}^{n}(\Delta z_i - \mu_z)^2\right]}. \tag{6}$$

The test for significant bias in the Z direction (elevation) is made by comparing the theoretical statistics ($t_{n-1,\alpha}$) from the tabled values to the sample statistic (t_{sample}) based on the equation:

$$t_{\mathrm{sample}} = \frac{\mu_z}{\sigma_z}\sqrt{n}. \tag{7}$$

If $|t_{\mathrm{sample}}| < t_{n-1,\alpha}$, then the tested DSM is accepted as free from bias in elevation.

Table 2
Residuals of X, Y and Z components and total residual for each model computed in the process of DSM extraction with distinct configurations of GCPs.

	DSM-1	DSM-2	DSM-3	DSM-4	DSM-5
GCPs	8	9	10	11	12
X residual (m)	0.795	0.754	0.734	0.710	0.796
Y residual (m)	0.541	0.573	0.546	0.538	0.500
Z residual (m)	0.539	0.518	0.509	0.493	0.514
Total residual (m)	1.103	1.080	1.047	1.018	1.072

The test for precision in elevation is made by comparing the theoretical statistic ($\chi^2_{n-1,\alpha}$) from the tabled values to the sample statistic χ^2 based on the equation:

$$\chi^2 = (n-1)\frac{s_z^2}{\sigma_z^2} \tag{8}$$

where s_z varies as a function of the map scale using the relation $\sigma_z = \mathrm{RMSE}$.

If $|\chi^2_{\mathrm{sample}}| < \chi^2_{n-1,\alpha}$, the DSM is accepted as meeting the accuracy standard for desired map scale.

The value of the RMSE for the PEC was previously discussed.

5. Results and discussion

Taking into account that the number of GCPs has direct influence on the DSM extraction and the quantity of ICPs on the estimation of the elevation accuracy, these two issues were also investigated. Selecting ground features with which to collect GCPs with number, quality, and distribution is a critical point for the operational use of the technology in the region. Natural ground features (clearings, outcrops, ridges, minor drainages, etc.) or anthropogenic targets (buildings, bridges, road intersections, agricultural field boundaries, etc.) are restricted or poorly expressed in SAR images for this kind of environment. In the case of GCPs, a larger number is recommended to improve accuracy for DSM extraction with samples ideally chosen on a variety of locations and ground elevations, particularly at the lowest and highest elevation. Conversely, ICPs also play a key role in quality control for mapping production, and a balance has to be reached between few ICPs, giving invalid accuracy estimation and an excessive number, providing a safe analysis with unrealistic cost. Thus, the strategy was to start with a minimum of 8 GCPs (monoscopic plotting) as required by the OrthoEngine software, and keeping a fixed number of 30 ICPs, roughly near the 28 ICPs as recommended in the literature. Additional GCPs were gradually added with the corresponding DSMs being analyzed regarding quality (presence of failed areas, blunders, etc.) and statistics (residual report errors on GCPs) up to the final combination using 12 GCPs and 30 ICPs for accuracy estimation. The GCPs residuals of the components X, Y and Z were computed, as well as the total residual of each model that was computed in the process of DSM extraction with distinct configuration of GCPs. The worst total residual value was 1.103 m, proving that Toutin's 3D Radargrammetric model has a good stability and robustness (Table 2). In addition, the X, Y residuals are indicators of the planimetric errors of the products, with values better than one third of the spatial resolution (better than 1 m).

A total of five DSMs with 12 m of pixel spacing were produced up to the final combination using 12 GCPs. From the 30 ICPs the z residual discrepancies (Δz_i) were computed for each extracted DSM. Table 3 presents z residual discrepancies for selected ICPs representatives of three distinct elevation intervals. It is important to mention that the residual discrepancies are indicators of the DSM offset to the real topography since the X-band SAR responses are mainly controlled by the top layer and the crown

Please cite this article in press as: Oliveira, C.G., et al., Assessment of radargrammetric DSMs from TerraSAR-X Stripmap images in a mountainous relief area of the Amazon region. ISPRS Journal of Photogrammetry and Remote Sensing (2010), doi:10.1016/j.isprsjprs.2010.08.008

Table 3
Z residual discrepancies (Δz_i) computed from TSX-SM DSMs and selected ICPs for three different elevation ranges.

Elevation range	Selected ICP	DSM-1 8GCPs	DSM-2 9GCPs	DSM-3 10GCPs	DSM-4 11GCPs	DSM-5 12GCPs
<300 m	11	13.35	13.35	12.35	13.35	13.35
	14	8.56	7.56	7.56	7.56	7.56
	28	8.41	6.41	7.41	7.41	7.41
300–600 m	13	−7.70	−7.70	−8.70	−8.70	−7.70
	23	−6.31	−9.31	−4.31	−5.31	−6.31
	29	−0.73	−2.73	−1.73	−1.73	−1.73
>600 m	1	−4.71	1.29	−0.71	−0.71	0.29
	7	−9.19	−10.19	−8.19	−8.19	−9.19
	26	5.92	5.92	6.92	5.92	5.92

Table 4
p-value results of the *Shapiro–Wilk* test of normality computed from z residual discrepancies (Δz_i) for all TSX-SM DSMs ($\alpha = 0.05$; $n = 30$).

DSMs	GCPs	p-values
DSM-1	8	0.502
DSM-2	9	0.476
DSM-3	10	0.056
DSM-4	11	0.067
DSM-5	12	0.122

Table 5
Test results for bias error and precision for TSX-SM DSMs from distinct GCPs numbers and 30 ICPs showing that all DSMs fulfilled the trend ($t_{\text{sample}} < t_{(n-1,5\%)}$) and precision ($\chi^2_{\text{sample}} < \chi^2_{(n-1,10\%)}$) requirements.

	DSM-1	DSM-2	DSM-3	DSM-4	DSM-5
GCPs	8	9	10	11	12
t_{sample}	0.393	0.345	0.128	0.042	0.261
χ^2_{sample}	29.465	28.358	26.597	27.181	28.642

of the trees. The variation of the residual discrepancies can be explained as follows: positive values are normally associated with measurements taken on roads and tracks along the forest (probably with DSM values more affected by the vegetation), while negative values are related to open areas (lateritic duricrusts, deforested areas, mining areas, etc.). In addition, histograms, normal probability plot of z residual discrepancies and the *Shapiro–Wilk* test (Table 4) were also carried out using the R statistic software (R Development Core Team, 2009) to verify the normality of residuals. The results of Table 4 (p-values > 0.05) supported the assumption of normality of residual discrepancies for all DSMs, which was confirmed through histograms and normal probability plots of the residuals. Then, the null hypothesis of the *Shapiro–Wilk* test can be accepted. The results for mean of discrepancies (μ_z), standard deviation (s_z) and RMSE values for all DSMs pointed out that the increase in the number of GCPs did not have significant impact on the derived products. The best RMSE value (6.279 m) was obtained from the stereo-model using 10 GCPs (Fig. 3) and the worst (6.625 m) case was with 8 GCPs. It is important to mention that the DSMs were extracted based on GCP plotting under monoscopic viewing and the use of stereo GCPs will improve the DSM accuracies, as previously reported in the literature (Toutin, 2000).

The test results for significant bias error and precision (Table 5) allowed important findings: (1) all the TerraSAR-X Stripmap DSMs fulfilled the trend requirements showing no bias since the t_{sample} values were smaller than the $t_{(n-1,5\%)}$ values, and (2) the comparison of χ^2_{sample} and $\chi^2_{(n-1,10\%)}$ values indicated that the DSMs are also compatible with the Brazilian PEC altimetric requirements for a 1:50,000 A Class Map (RMSE $\leq$ 6.67 m), independently of the number of GCPs that was used as input for the DSMs extraction.

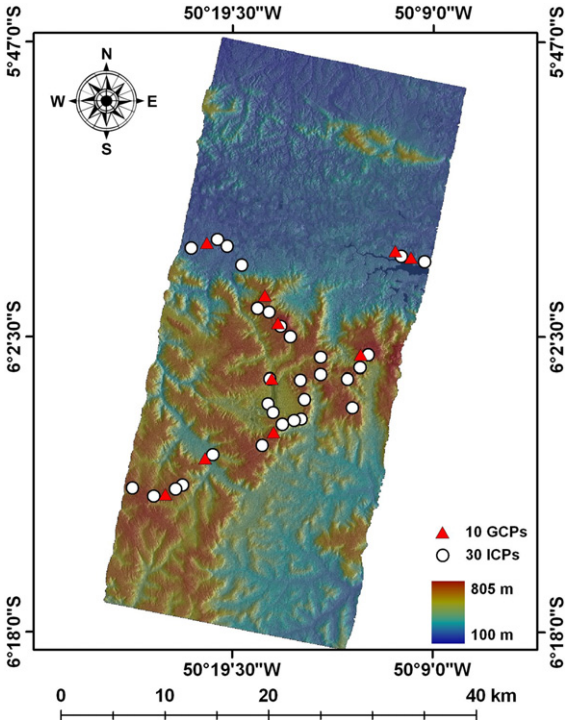

Fig. 3. TSX-SM DSM extracted with 10 GCPs (pseudo-color representation).

6. Conclusions

The investigation supports the conclusion that for similar environment (mountainous relief) of the Amazon region, radargrammetric DSMs produced from TerraSAR-X Stripmap images fulfill the Brazilian PEC requirements for 1:50,000 A Class Map. In addition, it was possible to conclude that TerraSAR-X Stripmap DSMs with RMSE errors less than 6.67 m can be obtained with a few GCPs numbers (minimum 8), which is also important considering the costs of GPS measurements for operational use in this kind of terrain. Further efforts will be necessary to evaluate the improvement of DSM accuracies using stereo GCP plotting, and also alternatives for deriving TerraSAR-X Stripmap DSMs, such as using distinct modeling, particularly based on calculated slant ranges and Doppler planes. Finally, it is important to mention that for cartographic production updated planimetric information is also necessary. Since TerraSAR-X also provides planimetric information, it can be a good alternative to overcome the critical lack of detailed topographic information in large areas of the Brazilian Amazon.

Acknowledgements

The authors would like to thank the referees for their critiques and suggestions that helped to improve the quality of the paper.

Please cite this article in press as: Oliveira, C.G., et al., Assessment of radargrammetric DSMs from TerraSAR-X Stripmap images in a mountainous relief area of the Amazon region. ISPRS Journal of Photogrammetry and Remote Sensing (2010), doi:10.1016/j.isprsjprs.2010.08.008

Special thanks to Infoterra GmbH (Germany) for providing the TerraSAR-X Stripmap images and Dr. Philip Cheng (PCI Geomatics) for access to the TSX module of OrthoEngine V10.1.4 software. The authors are also thankful to CAPES and CNPq for research grants received for the first and second authors during this investigation.

References

Fritz, T., Eineder, M., 2009. TerraSAR ground segment—basic product specification document. CAF—Cluster Applied Remote Sensing (TX-GS-DD-3302), Release 1.6, 18.03.2009, 108 p. http://sss.terrasar-x.dlr.de/pdfs/TX-GS-DD-3302.pdf (accessed 03.04.09).

Galo, M., Camargo, P.O., 1994. O uso do GPS no controle de qualidade de cartas. In: COBRAC-1994, 1° Congresso Brasileiro de Cadastro Técnico Multifinalitário. Tomo II. Florianópolis, Brazil. pp. 41–48.

Herrmann, J., Bottero, A.G., 2007. TerraSAR-X mission: the new generation in high resolution satellites. In: Proc. Brazilian Remote Sensing Symposium. Florianópolis, Brazil. pp. 7063–7070.

IBGE. 2002. Brazilian institute of geography and statistics, mapa índice digital: mapeamento geral do Brasil. 2nd ed. Rio de Janeiro, IBGE/DSG (on CD-ROM).

Kutner, M.H., Nachtsheim, C.J., Neter, J., Li, W., 2004. Applied Linear Statistical Models, fifth ed. McGraw-Hill, Irwin, New York.

Li, Z., Liu, G., Ding, X., 2006. Exploring the generation of digital elevation models from same-side ERS SAR images: topographic and temporal effects. Photogrammetric Record 21 (114), 124–140.

Maune, D.F. (Ed.), 2007. Digital Elevation Model Technologies and Applications: the DEM User Manual, second ed. American Society for Photogrammetry and Remote Sensing, ASPRS, Bethesda, Maryland.

Merchant, D.C., 1982. Spatial accuracy specification for large scale line maps. In: American Congress on Surveying and Mapping Annual Meeting, 42nd. Denver, CO. pp. 222–231.

Oliveira, C.G., Paradella, W.R., 2008. An assessment of the altimetric information derived from spaceborne SAR (RADARSAT-1, SRTM3) and optical (ASTER) data for cartographic application in the Amazon region. Sensors 8 (6), 3819–3829.

Oliveira, C.G., Paradella, W.R., 2009. Evaluating the quality of the digital elevation models produced from ASTER stereoscopy for topographic mapping in the Brazilian Amazon region. Annals of the Brazilian Academy of Sciences 81 (2), 217–225.

Ostrowski, J.A., Cheng, P., 2000. DEM extraction from stereo SAR satellite imagery. In: Geoscience and Remote Sensing Symposium Proceedings. IGARSS 2000. In: IEEE International, vol. 5. pp. 2176–2178.

Paradella, W.R., Bignelli, P.A., Veneziani, P., Pietsch, R.W., Toutin, T., 1997. Airborne and space-borne synthetic aperture radar (SAR) integration with Landsat TM and Gamma ray spectrometry for geological mapping in a tropical rain forest environment, the Carajás Mineral Province, Brazil. International Journal of Remote Sensing 18 (7), 1483–1501.

Paradella, W.R., Oliveira, C.G., Luiz, S., Cecarelli, I.C.F., Cottini, C.P., Okida, R., 2005. Operational use of RADARSAT-1 fine stereoscopy integrated with TM-landsat 5 data for cartographic application in the Brazilian Amazon. Canadian Journal of Remote Sensing 31 (2), 139–148.

Paradella, W.R., Silva, M.F.F., Rosa, N.A., Kushigbor, C.A., 1994. A geobotanical approach to the tropical rain forest environment of the Carajás Mineral Province (Amazon region, Brazil), based on digital TM-Landsat and DEM data. International Journal of Remote Sensing 15 (8), 1633–1648.

PCI Geomatics, 2007. Geomatica orthoengine 10.1 user guide PCI. Geomatics Enterprises Inc., Richmond Hill, Ontario, Canada, p. 179.

R Development Core Team, 2009. R: a language and environment for statistical computing. R Foundation for Statistical Computing, Vienna Austria, ISBN: 3-900051-07-0 (accessed 15.12.09) URL: http://www.R-project.org.

Schubart, H.O.R., 1989. Diagnosis of the natural resources of Amazonia. In: Amazônia: Facts, Problems and Solutions Symposium, vol. 1. São Paulo, Brazil. pp. 55–67.

Shaker, A., 2008. Satellite sensor modeling and 3D geo-positioning using empirical models. International Journal of Applied Earth Observation and Geoinformation 10 (3), 282–295.

Shapiro, S.S., Wilk, M.B., 1965. An analysis of variance test for normality (complete samples). Biometrika 52 (3–4), 591–611.

Toutin, T., 1998. Evaluation de la précision géométrique des images de RADARSAT. Canadian Journal of Remote Sensing 23 (1), 80–88.

Toutin, T., 1999. Error tracking of radargrammetric DEM from RADARSAT images. IEEE Transactions on Geoscience and Remote Sensing 37 (5), 2227–2238.

Toutin, T., 2000. Evaluation of radargrammetric DEM from RADARSAT images in high relief areas. IEEE Transactions on Geoscience and Remote Sensing 38 (2), 782–789.

Toutin, T., 2003. Path processing and block adjustment with RADARSAT-1 SAR images. IEEE Transactions on Geoscience and Remote Sensing 41 (10), 2320–2328.

Toutin, T., Carbonneau, Y., St-Laurent, L., 1992. An integrated method to rectify airborne radar imagery using DEM. Photogrammetric Engineering & Remote Sensing 58 (4), 417–422.

Toutin, T., Gray, L., 2000. State-of-the-art of elevation extraction from satellite SAR data. ISPRS Journal of Photogrammetry and Remote Sensing 55 (1), 13–33.

USGS. 1997. Standards for digital elevation model, part 3: quality control, US geological survey, Reston, Virginia, USA, 10 p. http://rockyweb.cr.usgs.gov/nmpstds/demstds.html (accessed 13.10.98).

Please cite this article in press as: Oliveira, C.G., et al., Assessment of radargrammetric DSMs from TerraSAR-X Stripmap images in a mountainous relief area of the Amazon region. ISPRS Journal of Photogrammetry and Remote Sensing (2010), doi:10.1016/j.isprsjprs.2010.08.008